A Thiomidazolylborate based Carbon Paste Electrode for Voltametric Detection of Heavy Metals in Wastewater

Gaber A.M. Mersal, Hamdy El-Sheshtawy, Ahmed Fallatah, Rabah Boukherroub, Mohammed Amin, Dalia Saleh, Mohamed Ibrahim

Asian Journal of Chemistry; Vol. 34, No. 3 (2022), 635-643

ASIAN JOURNAL OF CHEMISTRY

https://doi.org/10.14233/ajchem.2022.23580

A Thiomidazolylborate based Carbon Paste Electrode for Voltametric Detection of Heavy Metals in Wastewater

GABER A.M. MERSAL[1,*], HAMDY S. EL-SHESHTAWY[2], AHMED M. FALLATAH[1], RABAH BOUKHERROUB[3], MOHAMMED A. AMIN[1], DALIA I. SALEH[1] and MOHAMED M. IBRAHIM[1,*]

[1]Department of Chemistry, College of Science, Taif University, P.O. Box 11099, Taif 21944, Saudi Arabia
[2]Department of Chemistry, Faculty of Science, Kafr El-Sheikh University, Kafr El-Sheikh 33516, Egypt
[3]Univ. Lille, CNRS, Centrale Lille, Univ. Polytechnique Hauts-de-France, UMR 8520 - IEMN, F 59000 Lille, France

*Corresponding author: E-mail: gamersal@yahoo.com

Received: 11 October 2021; *Accepted*: 30 November 2021; *Published online*: 14 February 2022; AJC-20696

The ligand potassium hydro*tris*(N-(2,6-xylyl)-2-thioimidazolyl)borate (KTt^{xylyl}) was utilized to construct a carbon paste modified electrode (KTt^{xylyl}/CPE), which was studied using electrochemical impedance spectroscopy, cyclic voltammetry and square wave voltammetry (SWV). Its electrochemical response was investigated, and it demonstrated a significant improvement in the detection of both lead(II) and cadmium(II), allowing determination of lead(II) at trace concentrations. The spectroscopic evidence includes FT-IR, Raman, ^{1}H NMR and also DFT calculations using B3LYP/LANL2DZ level of theory indicate the high affinities of these ions toward the ligand forming lead(II) and cadmium complexes of the type [Tt^{xylyl}MCl]. Negative electrostatic potential of the tri(thione) donors deriving their binding abilities toward both ions. The detection limits based on 3(SD/m) were; 0.112 µM and 0.204 µM for lead(II) and cadmium(II), respectively. The simultaneous detection of these ions in several waste water samples was examined in order to verify the modified electrode. Data from the ICP-AES instrument was compared to the results obtained.

Keywords: Thioimidazolylborate, Modified CPE, Wastewater, Cyclic voltammetry, DFT calculations.

INTRODUCTION

One of the most important issues in our new world is the pollution of the atmosphere by trace heavy metals. Very low levels of trace heavy metal contamination are highly toxic to humans and animals. A difficult analytical concern is the identification of trace toxic heavy metal ions in multiple environmental samples. Lead(II) is considered one of the most harmful environmental toxins and even in the presence of low concentrations, has a potent chemical toxicity effect. Lead(II) is extremely harmful to the nervous, immune, gastrointestinal and reproductive systems in human and animal organs. In comparison, cadmium is one of the most highly toxic human heavy metals and carcinogenic compounds. It has been described as the sixth most dangerous material that endangers human health [1-3]. Human exposure to lower levels of cadmium can lead to renal dysfunction, bone degeneration, pulmonary insufficiency, liver injury and high blood pressure [4,5].

Therefore, considerable attention has been given to the creation of a highly sensitive method for the determination of trace quantities of heavy metals (especially Pb^{2+} and Cd^{2+}). Various methods, such as inductively coupled plasma mass spectroscopy (ICP-MS) [6-8]. X-ray florescence spectroscopy [9-12] and atomic adsorption spectroscopy (AAS) [13-18], have been used for the detection of Cd^{2+} and Pb^{2+}. These methods have excellent sensitivity and good selectivity, but they have various limitations, such as time-consuming analytical methods and they require expensive and complex equipment. Electrochemical methods including stripping voltammetric techniques such as anodic stripping voltammetry, cathodic stripping voltammetry, square wave voltammetry and differential pulse voltametry has been recognized as a powerful tool for measuring trace analysis [19-24]. For electrochemical methods, various advantages have been shown, such as fast analytical speed, higher selectivity and sensitivity, low coast and easy to operate. Due to various advantages such as easy processing,

non-toxic, reusable, rapid reaction, high selectivity, low detection limit, stability in different solvents, longer lifespan and low cost.

For the electrochemical detection of Cd^{2+} and Pb^{2+}, different chemically modified electrodes have been developed [25-31]. CPE is a chemically modified electrode,which is commonly used in voltammetric procedures. CPE is made by combining graphite powder with the necessary binder and a chemical known as a modifier to increase electrode selectivity. Some modifiers were utilized with CPE for the electrochemical estimation of Cd^{2+} and Pb^{2+} in the literature such as bismuth-modified zeolite [32], zeolite [33], hydroxyapatite [34], 1-furoylthioureas [35], organofunctionalized 2-benzothiazolethiol nanostructured silica SBA-15 [36] spent coffee grounds [37], Eu^{3+}-doped NiO [38], antimony oxide multiwall carbon nanotube electrode (Sb_2O_3/MWCNTs) [39], disodium ethylenediamine tetraacetic acid (EDTA) [40] and bismuth nanosheets modified screen-printed CE [41]. For the electrochemical detection of Cd^{2+} and Pb^{2+}, a tri(thione) containing ligand, potassium hydro*tris*(N-(2,6-xylyl)-2-thioimidazolyl)borate (KTt^{xylyl}) modified CPE was utilized.

EXPERIMENTAL

All reagents were of commercial quality and did not require further purification. Sigma-Aldrich provided graphite powder and paraffin wax. H_3BO_3, H_3PO_4, NaH_2PO_4, Na_2HPO_4 CH_3COOH, and NaOH were obtained from Merck. $Cd(NO_3)_2$ and $Pb(NO_3)_2$ were obtained from Riedel-de Haen AG Seelze-Hannover, Germany. The tri-thion ligand, KTt^{xylyl} was synthesized by our previously method [42].

Preparation of carbon paste electrode (CPE) and its modified CPE-KTt^{xylyl}: The bare CPE was developed by forcefully hand combining graphite powder (65%) and hot paraffin wax (35%) into an uniform paste. The paste was then placed into the end of an insulin syringe (ID: 2 mm). By pressing the copper wire under the syringe, an external electrical connection was created. KTt^{xylyl}-modified CPE was made by combining graphite powder (60%) with paraffin wax (30%) in the presence of various ligand KTt^{xylyl} ratios (1, 5 and 10%). Emery paper was used to polish the electrode surface, which was then thoroughly cleaned with deionized water.

Electrochemical studies: An Autolab potentiostat model PGSTAT 302, Eco Chemie, Utrecht, Netherlands, was used for the square wave and cyclic voltammetric experiments, which was powered by GPES. Eco Chemie, a program version 4.9. Electrochemical cells with three electrodes were employed. The working electrode was either bare CPE or modified CPE-KTt^{xylyl} electrodes, the reference electrode was SCE, and the counter electrode was platinum wire. Metrohom pH-meter with a composite glass electrode was used to measure the pH values. Heavy metal ion concentrations were determined using a Perkin-Elmer Optima 2100 Dual View ICP-AES apparatus linked to an AS 93 Plus Auto-sampler.

Computational details: The construction of the tri-thion KTt^{xylyl} and its Cd^{2+} and Pb^{2+} complexes were optimized with Gaussian 09. The optimized structures were envisioned using Gaussian view 6.1 version. The DFT calculations were completed using the B3LYP level of principle. The basis set 6-311++G-(d,p) was handled for C, S, B, N, and H atoms where the lanl2dz bases set was used for Cd and Pb atoms. In order to approve the minimum structure optimization, the frequency calculations were performed at the optimized structures where all frequencies were positive. TD-DFT calculations were performed to calculate the HOMO and LUMO boundary orbitals.

RESULTS AND DISCUSSION

Characterization of Tt^{xylyl} based cadmium(II) and lead(II) complexes: The microcrystalline lead and cadmium complexes were synthesized as reported earlier [42]. The Pb(II) and Cd(II) ions are coordinated to three thioimidazolyl thione sulfur atoms and one chloride atom in structurally pseudo-tetrahedral arrangements.

Electrochemical characterization of electrochemical sensor

Cyclic voltammetry: The electrochemistry of the CPE and the modified CPE-KT^{xylyl} electrodes was investigated thorough a potential range: +1.5 to -1.5 V (*vs.* SCE) using 50 mV s^{-1} scan rate in 5.0 mM $K_3[Fe(CN)_6]/K_4[Fe(CN)_6]$ in the presence of 1.0 M KCl. Fig. 1 illustrated the obtained cyclic voltammograms, the bare CPE showed one redox couple, in which the oxidation and cathodic peaks appeared at 0.59 and -0.30 V, respectively with a potential difference (ΔEp) of 890 mV [43]. Whereas the modified CPE-KTt^{xylyl} electrode, illustrated a specified redox system observed with oxidation and reduction peaks at +0.6 and 0.0 V, respectively, with a 600 mV potential difference.

The peak current in the modified CPE-KTt^{xylyl} electrode is markedly higher than in the bare CPE electrode as shown in Fig. 1. This might arise from adding the ligand KTt^{xylyl} as a modifier to CPE that stimulated the redox reaction as well as facilitated the rate of electron transfer [44]. This was evidenced by a considerable rise in peak current and a lowering the difference between the peak potential (Ep).

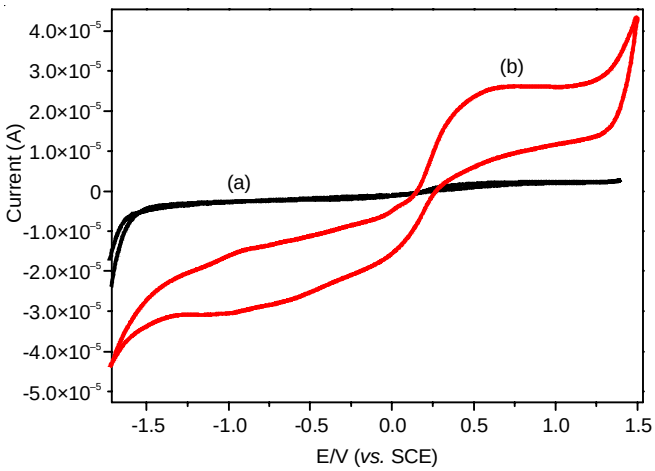

Fig. 1. Cyclic voltammetric response for (a) bare CPE and (b) CPE-KTt^{xylyl} modified electrodes in a solution containing 5.0 mM $[Fe(CN)_6]^{3-/4-}$ and 1.0 M KCl

Electrochemical impedance spectroscopic study: The electrical equivalent circuits for the modified CPE-KTt^{xylyl} electrode in the absence and presence of $[Fe(CN)_6]^{3-/4-}$ and KCl

(1 M) as an electrochemical redox system compatible with the impedance spectra are illustrated in Nyquist diagrams to obtain detailed information about the electrode solution interfaces. As shown in Fig. 2, the Nyquist diagrams, the bare CPE electrode (Fig. 2a) is a semi-circle domain with R_{ct} value of ~309.6 KΩ cm^2. Whereas in case of the modified CPE-KTt^{xylyl} electrode, the shape of Nyquist plot (Fig. 2b) is the same as that of the CPE, but with a smaller semicircle diameter and the value of R_{ct} is about 90.69 kΩ cm^2 [45].

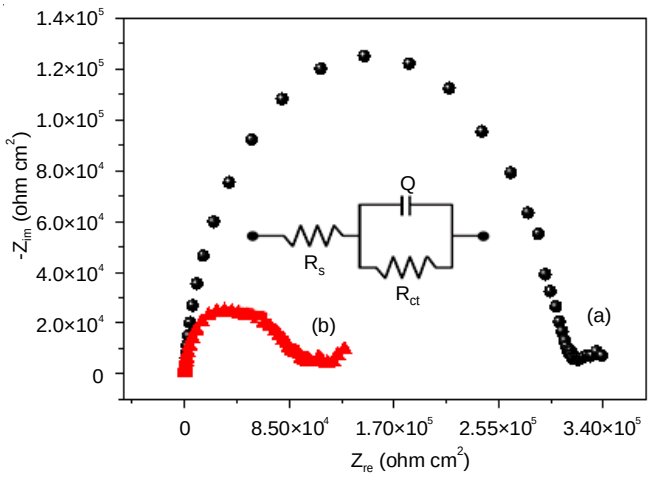

Fig. 2. Nyquist plots of CPE (a) and CP-KTt^{xylyl} modified electrode (b) in a solution containing 5 mM $[Fe(CN)_6]^{3-/4-}$ and 1 M KCl, (inset equivalent circuit for system). Inset: R_s (the solution/electrolyte resistance), Q a constant phase element corresponding to the double layer capacitance and R_{ct} is the charge transfer resistance associated with the oxidation of low valence mediator pieces

By comparing the polarization resistance of two electrodes, the results showed that the largest polarization resistance was obtained in the case of bare CPE. The lower R_{ct} on the surface of the modified CPE-KTt^{xylyl} electrode indicates that the ligand KTt^{xylyl} can enhance the electron transfer [46], thus speeding up the diffusion of the ferricyanide towards the electrode surface. Therefore, the conductivity was improved by modifying the CPE by KTt^{xylyl}.

Analysis for Pb^{2+} and Cd^{2+} ions

Cyclic voltammetry: The electrochemical behaviour of the CPE and CPE-KTt^{xylyl} modified electrodes in the absence and presence of 1×10^{-3} M Pb^{2+} and Cd^{2+} ions was investigated in an acetate buffer at pH 4.5 utilizing a potential range of -1.0 to +1.5 V (*vs.* SCE). In the case of bare CPE, no signals were appeared in the anode or cathode scan. Whereas, in the modified CPE-KTt^{xylyl} electrode, the Pb^{2+} ions showed a well defined oxidation peak at about -0.4 V (*vs.* SCE) and Cd^{2+} ions displayed a broad peak at about -0.6 V. Peak currents for Pb^{2+} and Cd^{2+} ions were considerably greater at the modified CPE-KTt^{xylyl} electrode than at the bared CPE. The influence of some supporting electrolytes for example: phosphate, sodium borate, acetate and Britton-Robinson buffers was further examined. Acetate buffer was selected for further determination of Pb^{2+} and Cd^{2+} ions using square wave voltammetry (SWV). The acetate buffer produced the finest peak shape and greatest peak current.

Square wave voltammetric studies:

Effect of pH: The electrochemical behaviour of Pb^{2+} (1.0×10^{-3} M) and Cd^{2+} (1.0×10^{-3} M) ions at the modified CPE-KTt^{xylyl} electrode was investigated by using different pH values (2.5 to 6.7) from acetate buffer at using square wave voltammetry (Fig. 3). The voltammograms showed a well separated peaks at all pH values under study. By increasing the pH values from 2.5 to 4.0, the oxidation peak currents for both Pb^{2+} and Cd^{2+} ions increased [47]. Upon increasing the pH higher than 4.0, the oxidation peak currents decreased. Because of this, the acetate buffer at pH 4.0 was selected.

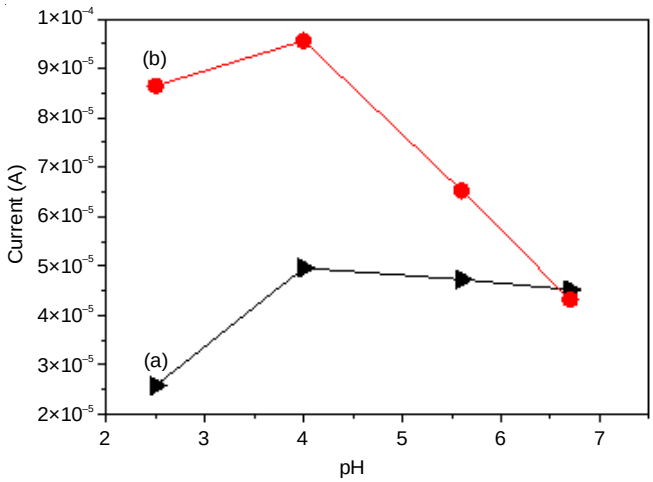

Fig. 3. Dependence of peak current height on pH for (a) 1×10^{-3} M Cd^{2+} and Pb^{2+} ions and a CPE-KTt^{xylyl} modified electrode

The SW anodic voltammograms for Pb^{2+} (1.0×10^{-3} M) and Cd^{2+} (1.0×10^{-3} M) ions at the modified CPE-KTt^{xylyl} electrode are shown in Fig. 4. In the case of bare CPE, no signals was observed. While in the modified CPE-KTtxylyl electrode, a well-defined and separated oxidation peaks were appeared for Pb^{2+} and Cd^{2+} ions at -0.44 and - 0.79 V (*vs.*SCE), respectively. This suggests that the presence of KTt^{xylyl} as a modifier plays a significant role in the accumulation of both Pb^{2+} and Cd^{2+} ions on the electrode surface and considerably improve the sensitivity for both ions detection [48]. The presence of KTt^{xylyl} on the surface of CPE improves the rate of metal pre-concentration from aqueous solution to the electrode surface *via* complex formation between Pb^{2+} or Cd^{2+} ions and the tri-thion donors KTt^{xylyl} (**Scheme-I**). The considerable difference in the oxidation peaks potentials (approximately 350 mV) between Pb^{2+} and Cd^{2+} ions implies that these ions might be determined simultaneously in water samples using the built modified electrode [49].

Influence of SWV variables: The influence of various SWV parameters on the peak height of Pb^{2+} (1.0×10^{-3} M) and Cd^{2+} (1.0×10^{-3} M) ions was studied. Fig. 5a displays the effect of SW frequency using various values from 8 to 26 Hz on the peak current of these ions. The results showed that the oxidation peak current increased to 12 and 14 Hz for Pb^{2+} and Cd^{2+} ions, respectively, after that the oxidation peak current decreased by the increase in frequency of square wave. For Pb^{2+} ions, a linear part was obtained from 8 to 12 Hz and for Cd^{2+} ions the

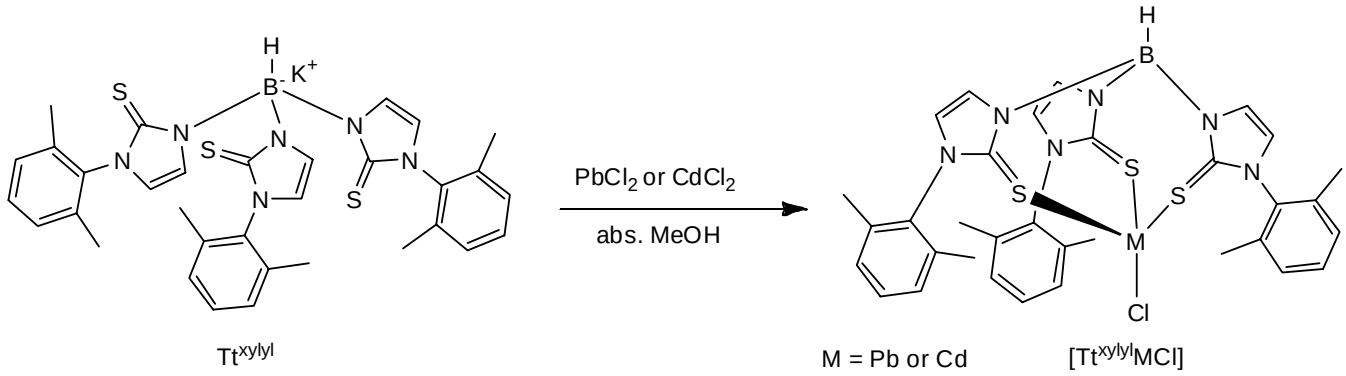

Tt^{xylyl} $[Tt^{xylyl}MCl]$

Scheme-I: Complex formation between M(II)[where M is, Pb or Cd] and KTt^{xylyl}

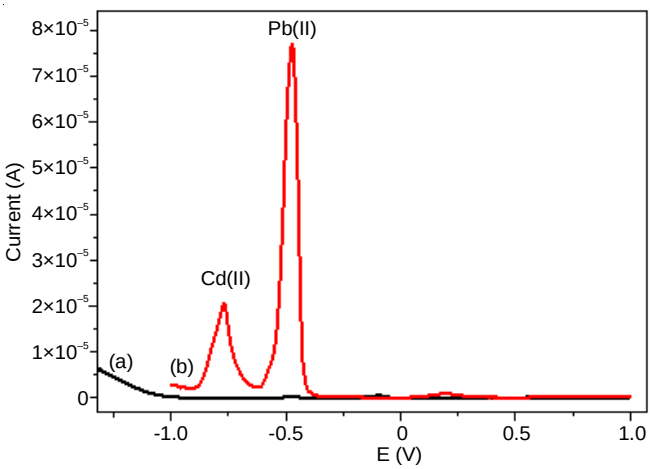

Fig. 4. Square wave voltammetric response for (a) Pb^{2+} (1.0×10^{-3} M) and Cd^{2+} (1.0×10^{-3} M) ions in acetate buffer (pH 4.0) at CPE and (b) and CPE-KTt^{xylyl} modified electrode

linear portion was obtained from 8 to 14 Hz. Fig. 5b indicates the effect of the SW pulse amplitude on the peak current of Pb^{2+} (1.0×10^{-3} M) and Cd^{2+} (1.0×10^{-3} M) ions using the 12 Hz SW frequency. The effect of SW pulse amplitude was examined from 1.0 to 100 mV. For Pb^{2+} the peak current increased with a linear from 1.0 to 50 mV and 60 mV for Cd^{2+}. Therefore, 50 mV the SW pulse amplitude was chosen to be the optimal height which be used for other investigations. The influence of step potential from 1.0-10 mV on the peak height of Pb^{2+} (1.0×10^{-3} M) and Cd^{2+} (1.0×10^{-3} M) ions is depicted. The peak current height increases linearly to 6 mV for Pb^{2+} and Cd^{2+} ions by increasing the step potential, after which the rise in peak height is not pronounced (Fig. 5c). As a result, a step potential of 6 mV was chosen for additional investigation [50].

Influence of initial potential: The influence of the initial potential on the current heights for both Pb^{2+} (1.0×10^{-3} M) and Cd^{2+} (1.0×10^{-3} M) ions was tested using (i) a potential range from -2.0 V to -0.1 V, (ii) 12 Hz SW frequency, (iii) 50 mV SW pulse amplitude, and (iv) 6 mV step potential. Fig. 6 shows that when the initial potential increases, the peak current for these ions decreases. As a result, a -1.6 V initial potential was chosen for future investigation and a lower baseline was detected.

Calibration plot and limit of detection: In order to evaluate the readability of the modified CPE-KTt^{xylyl} electrode using the following optimal conditions for the detection of both Pb^{2+} and Cd^{2+}: acetate (pH 4.0) as a supporting electrolyte, square wave parameters: 12 Hz frequency, 50 mV pulse amplitude and 6 mV step potential. The dependence of oxidation peak current on Pb^{2+} and Cd^{2+} ions concentration (1.0×10^{-6} M to 1.0×10^{-4} M) was examined. The results showed that two linear ranges were observed in the resulting calibration curve (i) from 1×10^{-6} to 5×10^{-5} M with a correlation coefficient of 0.9921 and 0.9744 and a relative standard deviation (RSD) of 6.506 $\times 10^{-8}$ and 3.0410^{-8} (Fig. 7a); (ii) from 1×10^{-5} to 1×10^{-4} M with a correlation coefficient of 0.985and 0.8998 and a RSD of 4.525×10^{-7} and 1.1908^{-7} M for Pb^{2+} and Cd^{2+} ions, respectively (Fig. 7b). The lower limit of detection for Pb^{2+} and Cd^{2+}

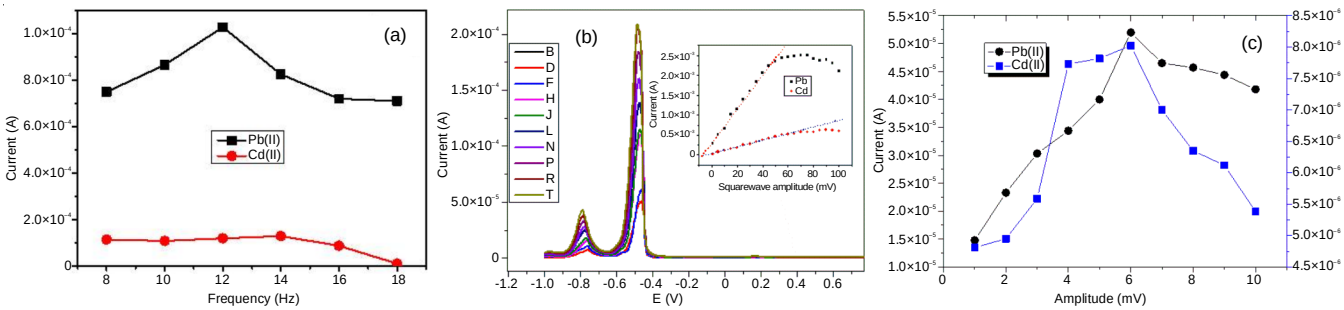

Fig. 5. (a) Dependence of square wave frequency on the peak current of 1×10^{-3} M Pb^{2+} and Cd^{2+} using different values from 8 to 18 Hz, (b) Dependence of square wave pulse amplitude on the peak current of 1×10^{-3} M Pb^{2+} and Cd^{2+} using 12 Hz square wave frequency. The pulse amplitude from 1.0 to 100 mV, (c) Influence of step potential (1-10 mV) on the peak height of Pb^{2+} (1.0×10^{-3} M) and Cd^{2+} (1.0×10^{-3} M) ions using 12 Hz square wave frequency and 50 mV square wave pulse amplitude

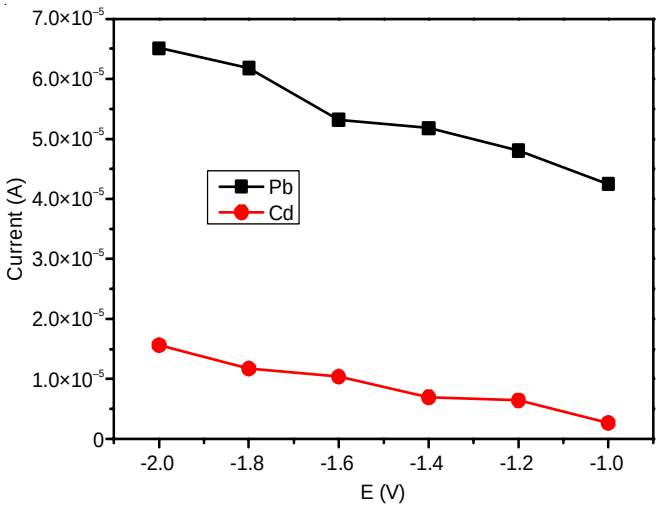

Fig. 6. Dependence of initial potential on the peak current height for 1 × 10^{-3} M Pb^{2+} and Cd^{2+} ions

ions were calculated and found to be 1.12 × 10^{-7} and 2.04 × 10^{-7} M for Pb^{2+} and Cd^{2+} ions, respectively. The obtained LOD for Cd(II) and Pb(II) using modified CPE-KTt^{xylyl} electrode was compared with some different modified electrodes for the simultaneous determination of Cd(II) and Pb(II) ions, the data summarized in Table-1.

Reproducibility: To evaluate the repeatability of the prepared electrode under consideration, ten successive measurements were taken using the ideal circumstances specified above to study the obtained peak current of Pb^{2+} (1.0 × 10^{-4} M) and Cd^{2+} (1.0 × 10^{-4} M) ions. The RSD was also calculated and determined to be 3.94 %. This indicates that the results obtained are well reproducible by this method.

Interferences studies: The effect of different metal ions on the simultaneous identification of Pb^{2+} (1.0 × 10^{-5} M) and Cd^{2+} (1.0 × 10^{-5} M) ions has been studied. The metal ions under investigation were Hg^{2+}, Zn^{2+}, Fe^{2+}, Mg^{2+}, Al^{3+}, Cu^{2+}, Ni^{2+} and Mn^{2+}. The added metal ion concentrations ranged from 1 × 10^{-4} to 1 × 10^{-3} M. A minor error of around ±7% was found at all concentrations tested.

Analytical applications: The proposed approach for determining Pb(II) and Cd(II) in water samples was used to investigate the validity of the produced CPE modified by KTt^{xylyl}. The results obtained are summarized in Table-2 using the optimal conditions and the calibration curve.

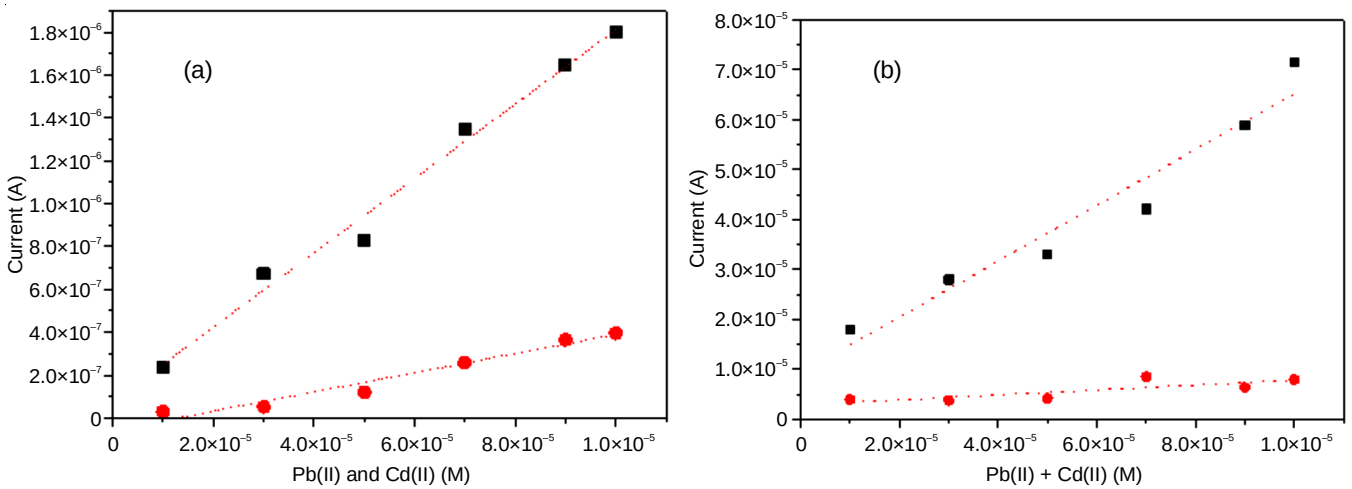

Fig. 7. Calibration curve for Pb^{2+} and Cd^{2+} ions using a two different concentration ranges: a) from 1 × 10^{-6} M to 1 × 10^{-5} M and b) form 1 × 10^{-5} M to 1 × 10^{-4} M using the optimal conditions mentioned before

TABLE-1
COMPARISON OF DIFFERENT MODIFIED ELECTRODES FOR THE SIMULTANEOUS DETERMINATION OF Pb(II) AND Cd(II)

Method	Electrode	Limit of detection (L)		Ref.
		Cd(II)	Pb(II)	
DPASV	$Mo_6S_xI_{9-x}$NWs/GCE	8.90 × 10^{-10}	2.20 × 10^{-9}	[51]
ASV	G/PANI/PS fiber with nanoporous/SPCE	3.90 × 10^{-8}	1.60 × 10^{-8}	[52]
DPASV	Bi/G/MWCNTs/GCE	8.90 × 10^{-10}	9.60 × 10^{-10}	[53]
SWASV	Bi/HP-β-CD-rGO/Nafion/GCE	0.07 × 10^{-9}	0.09 × 10^{-9}	[54]
SWASV	PPh_3/MWCNTs/1L/CPE	7.40 × 10^{-11}	6.00 × 10^{-11}	[55]
SWASV	SnO_2/rGO nanocomposite/GCE	1.02 × 10^{-10}	1.84 × 10^{-10}	[56]
DPASW	P(DPA-*co*-2ABN)	2.27 × 10^{-9}	7.96 × 10^{-10}	[57]
SWASV	Bi/Nafion/PANI-thiol/GCE	3.55 × 10^{-10}	2.40 × 10^{-10}	[58]
SWASV	PANI/GCEs	1.30 × 10^{-7}	1.00 × 10^{-7}	[59]
DPASV	Bi/Nafion/PDMcT-MWCNTs/GCE	2.70 × 10^{-10}	2.70 × 10^{-10}	[60]
DPSV	Bi/Nafion/PDMcT-MWCNTs/GCE	1.78 × 10^{-9}	4.80 × 10^{-10}	[61]
DPSV	Bi/ABTS-MWCNTs/GCE	1.60 × 10^{-10}	4.80 × 10^{-10}	[62]
DPSV	MWCNTs-NA/Bi	1.20 × 10^{-10}	3.50 × 10^{-10}	[63]
SWAV	Ti/CPE	2.83 × 10^{-7}	1.15 × 10^{-7}	This work

TABLE-2
Pb(II)/Cd(II) DETECTION IN WASTEWATER SAMPLES BY MEANS OF THE SUGGESTED PROCEDURE (n = 5) AND THE REFERENCE METHOD, ICP-AES INSTRUMENT

Pb(II) and Cd(II) [M] added	Pb(II) [M] found			Cd(II) [M] found		
	Proposed method	CP-AES	Relative error (%)	Proposed method	CP-AES	Relative error (%)
1×10^{-6}	0.90×10^{-6}	0.93×10^{-6}	- 3.22	0.89×10^{-6}	0.93×10^{-6}	-4.30
3×10^{-6}	2.92×10^{-6}	3.02×10^{-6}	-.331	2.51×10^{-6}	2.74×10^{-6}	8.39
5×10^{-6}	5.60×10^{-6}	5.2×10^{-6}	7.14	5.27×10^{-6}	5.01×10^{-6}	5.19
7×10^{-6}	7.33×10^{-6}	7.12×10^{-6}	2.8	7.26×10^{-6}	6.83×10^{-6}	6.29
9×10^{-6}	9.84×10^{-6}	9.25×10^{-6}	6.38	1.00×10^{-5}	9.74×10^{-6}	2.66
1×10^{-5}	1.09×10^{-5}	1.02×10^{-5}	6.86	1.35×10^{-5}	1.49×10^{-5}	-9.39
3×10^{-5}	2.69×10^{-5}	2.86×10^{-5}	-5.9	3.15×10^{-5}	3.34×10^{-5}	-5.68
5×10^{-5}	5.35×10^{-5}	5.13×10^{-5}	4.29	5.53×10^{-5}	5.22×10^{-5}	5.94
7×10^{-5}	7.68×10^{-5}	7.29×10^{-5}	5.34	7.90×10^{-5}	7.25×10^{-5}	8.96
9×10^{-5}	9.74×10^{-5}	9.17×10^{-5}	6.21	9.67×10^{-5}	9.14×10^{-5}	5.79
1×10^{-4}	1.11×10^{-4}	1.03×10^{-4}	8.0	1.25×10^{-4}	$1.14x\ 0^{-4}$	9.65

To validate the improved electrode's dependability, the analyzed wastewater samples were also assessed using ICP-AES as a reference technique. The outcomes obtained had been introduced in Table-1. The measurements records confirmed a properly settlement with these received by ICP-AES for detection of wastewater samples [64]. Wastewater samples were also assessed using ICP-AES, an independent standard method, to test the dependability of the new electrode. Table-1 displays the results collected. For the analyzed wastewater samples, the measurement values agreed well with those obtained by normal ICP-AES.

Computational studies: The structure of the complexes further explored by the DFT calculations. The optimized structure of KTt^{xylyl} by DFT calculations are shown in Fig. 8a. The *N*-(2-methylphenyl)-2-thioimid-azol-1-yl is coordinated with the boron (B) to form the hydrotris[*N*-(2-methylphenyl)-2-thioimid-azol-1-yl)borate through three B-N bonds (d = 1.55 Å and N-B-N = 117°). The calculated molecular electrostatic surface potential (MESP) of KTti shows that the negative charge is centered at the S core atoms (V = -3.4 kcal/mol), which is the potential site for the coordination with metal ions (Fig. 8b). The metal ions binding site is confirmed by the HOMO

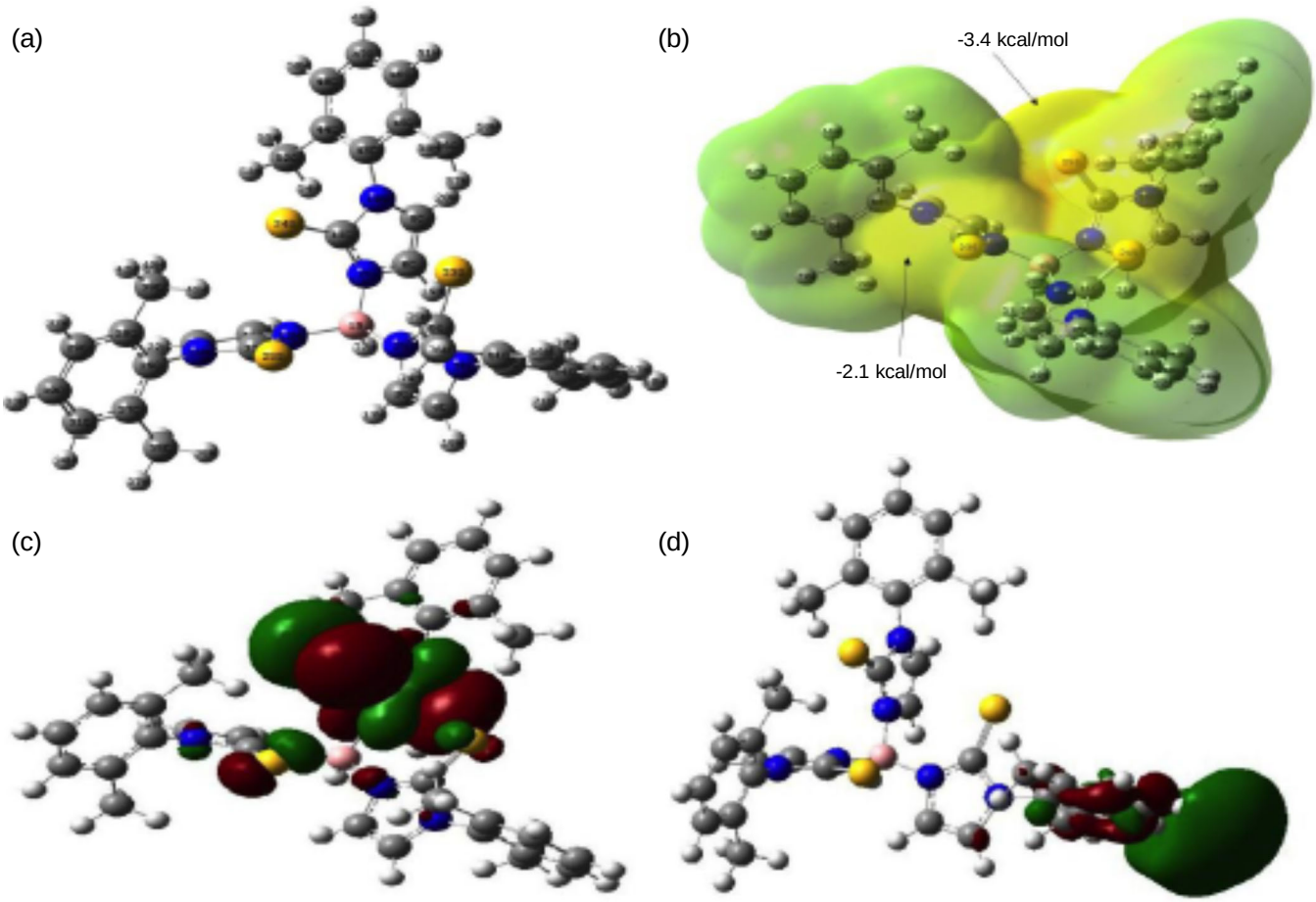

Fig. 8. (a) Optimized structure, (b) MESP, (c) HOMO and (d) LUMO of KTt^{xylyl} calculated at B3lyp/lanl2dz level of theory in the gas phase

and LUMO calculations (Fig. 8c-d) [65]. The HOMO orbitals (-2.01 eV) is situated on the C=S bond that participate in the metal coordination.

Fig. 9a shows the optimized structure of **2**, where Cd atom was coordinated with three S atoms (-C=S(23,24,25)···Cd70, 2.70 Å and 98.8º). The Cd atom was coordinated with Cl anion and bond length Cd70-Cl79 was 2.46 Å. The MESP of **2** shows the presence of high electron density on the halogen atom Cl (V = -31.2 kcal/mol). The calculations (DFT) showed that both HOMO (-0.80 eV) and LUMO (-0.61 eV) of **2** situated on the coordination site (Cd-Cl) position.

On the other hand, complex **1** show slightly elongated C=S bond upon coordination with the Pb cation (1.78 Å) (Fig. 10). The coordinated Pb cation with thione group showed different bond lengths. The C=S25···Pb70 bond length was 3.21 Å, however C=S24···Pb70 and C=S23···Pb70 showed 2.85 Å and 2.79 Å, respectively. The structure was distorted when one Cl atom was coordinated. This was due to the presence of vacant *d*-orbitals on Pb atom. Both HOMO (-5.22 eV) and LUMO (-1.17) positioned on the coordination site (Pb···Cl). After coordination of two Cl atoms with Pb atom, the C=S25···Pb70, C=S24···Pb70 and C=S23···Pb70 was 3.45 Å, 2.93 Å and 3.35

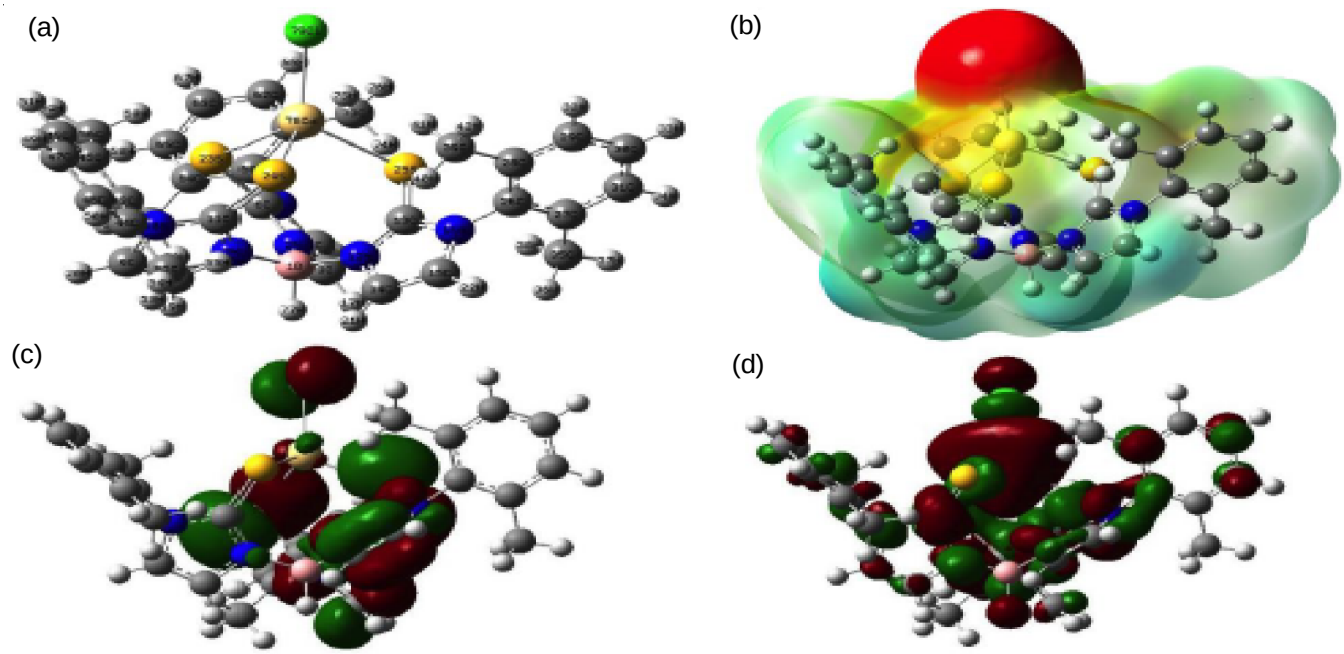

Fig. 9. (a) Optimized structure, (b) MESP, (c) HOMO and (d) LUMO of [(Tt^{xylyl}CdCl] complex in the gas phase

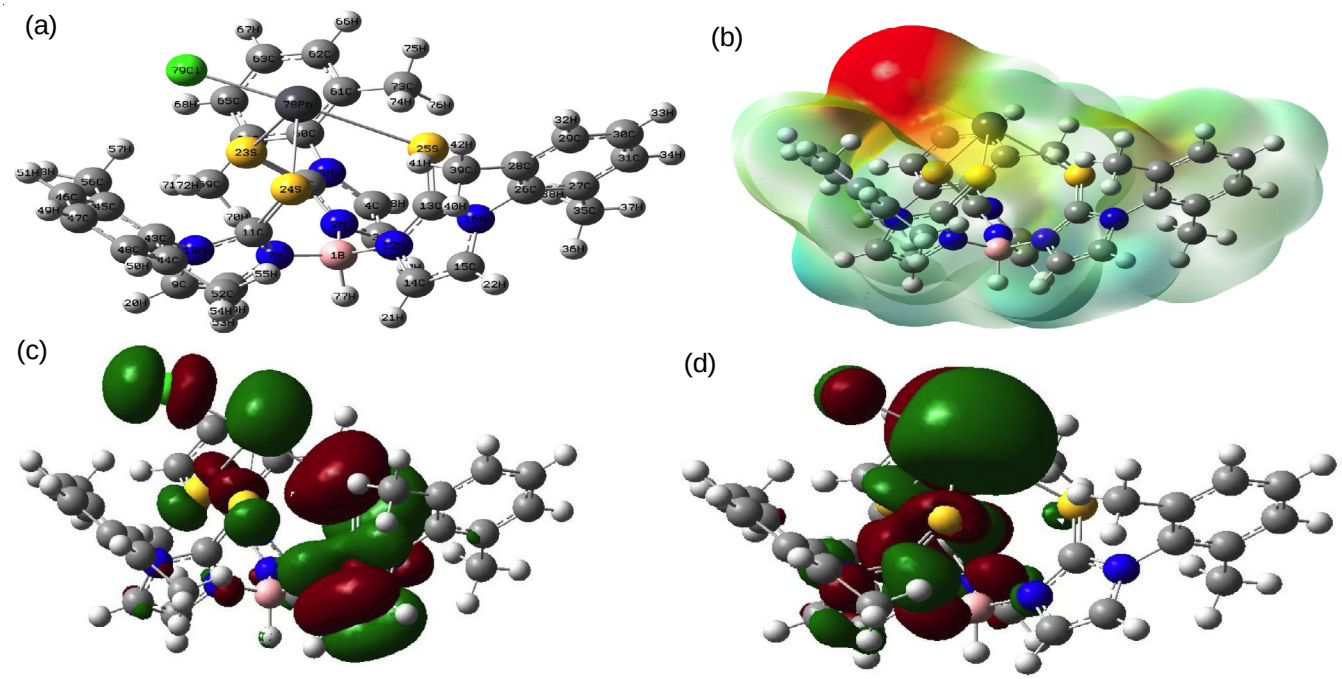

Fig. 10. (a) Optimized structure, (b) MESP, (c) HOMO and (d) LUMO of [Tt^{xylyl}PbCl] complex in the gas phase

Å, respectively. The MESP of the complexes show the increase negative charge on the two Cl atoms (V= -41.6 kcal/mol).

Conclusion

The tri-thion containing ligand namely, potassium hydro-*tris*(N-(2,6-xylyl)-2-thioimidazolyl)borate (KTt^{xylyl}) was used for the improvement of bare CPE for the simultaneous determination of Pb^{2+} (1.0×10^{-3} M) and Cd^{2+} (1.0×10^{-3} M) ions by SWV. The electrochemistry of the modified KTt^{xylyl} CPE eelectrode was characterized by EIS and CV. For the detection of Pb^{2+} and Cd^{2+} ions in wastewater using SWV, the influence of various experimental parameters was evaluated to obtain a maximum current peak. The affinity of the modified CPE towards these ions has also been confirmed separately via the synthesis of $[Tt^{xylyl}MCl]$ (M = Pb^{2+} and Cd^{2+}] complexes,which were characterized by FT-IR, Raman and ^{1}H NMR spectroscopies, as well as DFT calculation using B3LYP/LANL2DZ level of theory.

ACKNOWLEDGEMENTS

This research was funded by the University of Taif, Saudi Arabia, Deanship of Scientific Research, project No. 1-439-6070.

CONFLICT OF INTEREST

The authors declare that there is no conflict of interests regarding the publication of this article.

REFERENCES

1. A. Karimi, A. Naghizadeh, H. Biglari, R. Peirovi, A. Ghasemi and A. Zarei, *Environ. Sci. Pollut. Res. Int.*, **10**, 10317 (2020); https://doi.org/10.1007/s11356-020-07642-6
2. E. Margui, C. Fontas, M. Hidalgo and I. Queralt, *Spectrochim. Acta B Atom. Spectr.*, **63**, 1329 (2008); https://doi.org/10.1016/j.sab.2008.08.002
3. J. Li, S. Guo, Y. Zhai and E. Wang, *Anal. Chim. Acta*, **649**, 196 (2009); https://doi.org/10.1016/j.aca.2009.07.030
4. M. Iqbal, A. Saeed and S.I. Zafar, *J. Hazard. Mater.*, **148**, 47 (2007); https://doi.org/10.1016/j.jhazmat.2007.02.009
5. O.T. Ore and A.O. Adeola, *Energy Ecol. Environ.*, **6**, 81 (2021); https://doi.org/10.1007/s40974-020-00196-w
6. A. Ataro, R.I. McCrindle, B.M. Botha, C.M.E. McCrindle and P.P. Ndibewu, *Food Chem.*, **111**, 243 (2008); https://doi.org/10.1016/j.foodchem.2008.03.056
7. A. Milne, W. Landing, M. Bizimis and P. Morton, *Anal. Chim. Acta*, **665**, 200 (2010); https://doi.org/10.1016/j.aca.2010.03.027
8. N.S. Medvedev, A.V. Volzhenin and A.I. Saprykin, *Microchem. J.*, **157**, 104970 (2020); https://doi.org/10.1016/j.microc.2020.104970
9. Ö. Sögüt, T. Bali, H. Baltas and G. Apaydin, *Asian J. Chem.*, **25**, 4385 (2013); https://doi.org/10.14233/ajchem.2013.13985
10. O. Lau and S. Ho, *Anal. Chim. Acta*, **280**, 269 (1993); https://doi.org/10.1016/0003-2670(93)85131-3
11. N.M. Hepp, *J. AOAC Int.*, **103**, 1264 (2020); https://doi.org/10.1093/jaoacint/qsaa025
12. M. Tiwari, S.K. Sahu, T.D. Rathod, R.C. Bhangare, P.Y. Ajmal and A. Vinod Kumar, *J. Radioanal. Nucl. Chem.*, **325**, 751 (2020); https://doi.org/10.1007/s10967-020-07187-5
13. J.M. Jurado, M.J. Martín, F. Pablos, A. Moreda-Pineiro and P. Bermejo-Barrera, *Food Chem.*, **101**, 1296 (2007); https://doi.org/10.1016/j.foodchem.2006.01.027
14. H. Bagheri, A. Afkhami, M. Saber-Tehrani and H. Khoshsafar, *Talanta*, **97**, 87 (2012); https://doi.org/10.1016/j.talanta.2012.03.066
15. B.T. Zaman, A.F. Erulas, D.S. Chormey and S. Bakirdere, *Food Chem.*, **303**, 125396 (2020); https://doi.org/10.1016/j.foodchem.2019.125396
16. N. Jaiswal, C.M. Pandey, S. Solanki, I. Tiwari and B.D. Malhotra, *Mikrochim. Acta*, **187**, 1 (2020); https://doi.org/10.1007/s00604-019-3921-8
17. O. Yagci, E. Akkaya and S. Bakirdere, *Environ. Monit. Assess.*, **192**, 583 (2020); https://doi.org/10.1007/s10661-020-08548-z
18. J. Jiang, Z. Li, Y. Wang, X. Zhang, K. Yu, H. Zhang, J. Zhang, J. Gao, X. Liu, H. Zhang, W. Wu and N. Li, *Food Chem.*, **310**, 125824 (2020); https://doi.org/10.1016/j.foodchem.2019.125824
19. A. Sánchez, S. Morante-Zarcero, D. Pérez-Quintanilla, I. Sierra and I. del Hierro, *Sens. Actuators B Chem.*, **163**, 38 (2012); https://doi.org/10.1016/j.snb.2011.12.042
20. T. Hezard, K. Fajerwerg, D. Evrard, V. Collière, P. Behra and P. Gros, *J. Electroanal. Chem.*, **664**, 46 (2012); https://doi.org/10.1016/j.jelechem.2011.10.014
21. H. Li, J. Li, Z. Yang, Q. Xu, C. Hou, J. Peng and X. Hu, *J. Hazard. Mater.*, **191**, 26 (2011); https://doi.org/10.1016/j.jhazmat.2011.04.020
22. S. Abbasi, K. Khodarahmiyan and F. Abbasi, *Food Chem.*, **128**, 254 (2011); https://doi.org/10.1016/j.foodchem.2011.02.067
23. Z. Khalifa, K. Hassan, M.F. Abo Oura, A. Hathoot and M.A. Azzem, *ACS Omega*, **5**, 18950 (2020); https://doi.org/10.1021/acsomega.0c02228
24. E. Vlachou, A. Margariti, G.S. Papaefstathiou and C. Kokkinos, *Sensors*, **20**, 4442 (2020); https://doi.org/10.3390/s20164442
25. S. Liu and X. Zhang, *Int. J. Electrochem. Sci.*, **15**, 9838 (2020); https://doi.org/10.20964/2020.10.75
26. K. Tyszczuk-Rotko, R. Metelka and K. Vytøas, *Electrochim. Acta*, **92**, 335 (2013); https://doi.org/10.1016/j.electacta.2013.01.046
27. J. Ping, Y. Wang, J. Wu and Y. Ying, *Food Chem.*, **151**, 65 (2014); https://doi.org/10.1016/j.foodchem.2013.11.026
28. M.A.E. Mhammedi, M. Achak, M. Hbid, M. Bakasse, T. Hbid and A. Chtaini, *J. Hazard. Mater.*, **170**, 590 (2009); https://doi.org/10.1016/j.jhazmat.2009.05.024
29. M.F. Philips, A.I. Gopalan and K. Lee, *J. Hazard. Mater.*, **46**, 237 (2012); https://doi.org/10.1016/j.jhazmat.2012.07.069
30. M. Malakootian, S. Hamzeh and H. Mahmoudi-Moghaddam, *Microchem. J.*, **158**, 105194 (2020); https://doi.org/10.1016/j.microc.2020.105194
31. J. Pizarro, R. Segura, D. Tapia, F. Navarro, F. Fuenzalida and M. Jesús Aguirre, *Food Chem.*, **321**, 126682 (2020); https://doi.org/10.1016/j.foodchem.2020.126682
32. L. Cao, J. Jia and Z. Wang, *Electrochim. Acta*, **53**, 2177 (2008); https://doi.org/10.1016/j.electacta.2007.09.024
33. S. Senthilkumar and R. Saraswathi, *Sens. Actuators B Chem.*, **141**, 65 (2009); https://doi.org/10.1016/j.snb.2009.05.029
34. M.A. El Mhammedi, M. Achak and A. Chtaini, *J. Hazard. Mater.*, **161**, 55 (2009); https://doi.org/10.1016/j.jhazmat.2008.03.057
35. O. Estévez-Hernández, I. Naranjo-Rodríguez, J.L. Hidalgo-Hidalgo de Cisneros and E. Reguera, *Sens. Actuators B Chem.*, **123**, 488 (2007); https://doi.org/10.1016/j.snb.2006.09.030
36. I. Cesarino, G. Marino, J.R. Matos and E.T.G. Cavalheiro, *Talanta*, **75**, 15 (2008); https://doi.org/10.1016/j.talanta.2007.06.032
37. J. Estrada-Aldrete, J.M. Hernández-López, A.M. García-León, J.M. Peralta-Hernández and F.J. Cerino-Córdova, *J. Electroanal. Chem.*, **857**, 113663 (2020); https://doi.org/10.1016/j.jelechem.2019.113663

38. M. Malakootian, H. Abolghasemi and H. Mahmoudi-Moghaddam, *J. Electroanal. Chem.*, **876**, 114474 (2020); https://doi.org/10.1016/j.jelechem.2020.114474
39. T.L. Hai, L.C. Hung, T.T.B. Phuong, B.T.T. Ha, B.-S. Nguyen, T.D. Hai and V.-H. Nguyen, *Microchem. J.*, **153**, 104456 (2020); https://doi.org/10.1016/j.microc.2019.104456
40. C. Laghlimi, Y. Ziat, A. Moutcine, M. Hammi, Z. Zarhri, R. Maallah, O. Ifguis and A. Chtaini, *Chem. Data Collect.*, **29**, 100496 (2020); https://doi.org/10.1016/j.cdc.2020.100496
41. N.N. Ghazali, N.M. Nor, K.A. Razak, Z. Lockman, T. Hattori, *J. Nanopart. Res.*, **22**, 211 (2020); https://doi.org/10.1007/s11051-020-04946-z
42. M.M. Ibrahim, M. Shu and H. Vahrenkamp, *Eur. J. Inorg. Chem.*, **2005**, 1388 (2005); https://doi.org/10.1002/ejic.200400994
43. R. Cui, X. Wang, G. Zhang and C. Wang, *Sens. Actuators B Chem.*, **161**, 1139 (2012); https://doi.org/10.1016/j.snb.2011.11.040
44. S.M. Jones and E.I. Solomon, *Cell. Mol. Life Sci.*, **72**, 869 (2015); https://doi.org/10.1007/s00018-014-1826-6
45. B. Mei, O. Munteshari, J. Lau, B. Dunn and L. Pilon, *J. Phys. Chem. C*, **122**, 194 (2018); https://doi.org/10.1021/acs.jpcc.7b10582
46. M.D. Raicopol, A.M. Pandele, C. Dascălu, E. Vasile, A. Hanganu, G.-G. Vasile, I.G. Bugean, C. Pirvu, G. Stanciu and G.-O. Buica, *Sensors*, **20**, 6799 (2020); https://doi.org/10.3390/s20236799
47. S. Chairam, W. Sriraksa, M. Amatatongchai and E. Somsook, *Sensors*, **11**, 10166 (2011); https://doi.org/10.3390/s111110166
48. N.M. Thanh, N.D. Luyen, T.T.T. Toan, N. Hai Phong and N.V. Hop, *J. Anal. Methods Chem.*, **2019**, 1 (2019); https://doi.org/10.1155/2019/4593135
49. Y. Li, X. Liu, Z. Zeng, Y. Liu, X. Liu, W. Wei and S. Luo, *Sens. Actuators B Chem.*, **139**, 604 (2009); https://doi.org/10.1016/j.snb.2009.03.045
50. A.J. Borrill, N.E. Reily and J.V. Macpherson, *Analyst*, **144**, 6834 (2019); https://doi.org/10.1039/C9AN01437C
51. H. Lin, M. Li and D. Mihailovic, *Electrochim. Acta*, **154**, 184 (2015); https://doi.org/10.1016/j.electacta.2014.12.087
52. N. Promphet, P. Rattanarat, R. Rangkupan, O. Chailapakul and N. Rodthongkum, *Sens. Actuators B Chem.*, **207**, 526 (2015); https://doi.org/10.1016/j.snb.2014.10.126
53. H. Huang, T. Chen, X. Liu and H. Ma, *Anal. Chim. Acta*, **852**, 45 (2014); https://doi.org/10.1016/j.aca.2014.09.010
54. M. Lv, X. Wang, J. Li, X. Yang, C. Zhang, J. Yang and H. Hu, *Electrochim. Acta*, **108**, 412 (2013); https://doi.org/10.1016/j.electacta.2013.06.099
55. H. Bagheri, A. Afkhami, H. Khoshsafar, M. Rezaei and A. Shirzadmehr, *Sens. Actuators B Chem.*, **186**, 451 (2013); https://doi.org/10.1016/j.snb.2013.06.051
56. Y. Wei, C. Gao, F. Meng, H. Li, L. Wang, J.-H. Liu and X.-J. Huang, *J. Phys. Chem. C*, **116**, 1034 (2012); https://doi.org/10.1021/jp209805c
57. L. Chen, Z. Su, X. He, Y. Liu, C. Qin, Y. Zhou, Z. Li, L. Wang, Q. Xie and S. Yao, *Electrochem. Commun.*, **15**, 34 (2012); https://doi.org/10.1016/j.elecom.2011.11.021
58. Z. Wang, E. Liu and X. Zhao, *Thin Solid Films*, **519**, 5285 (2011); https://doi.org/10.1016/j.tsf.2011.01.176
59. X. He, Z. Su, Q. Xie, C. Chen, Y. Fu, L. Chen, Y. Liu, M. Ma, L. Deng, D. Qin, Y. Luo and S. Yao, *Michrochem. Acta*, **173**, 95 (2011); https://doi.org/10.1007/s00604-010-0541-8
60. X. Jia, J. Li and E. Wang, *Electroanalysis*, **22**, 1682 (2010); https://doi.org/10.1002/elan.201000083
61. W. Deng, Y. Tan, Z. Fang, Q. Xie, Y. Li, X. Liang and S. Yao, *Electroanalysis*, **21**, 2477 (2009); https://doi.org/10.1002/elan.200900207
62. H. Xu, L. Zeng, S. Xing, Y. Xian, G. Shi and L. Jin, *Electroanalysis*, **24**, 2655 (2008); https://doi.org/10.1002/elan.200804367
63. G. Zhao, Y. Yin, H. Wang, G. Liu and Z. Wang, *Electrochim. Acta*, **220**, 267 (2016); https://doi.org/10.1016/j.electacta.2016.10.059
64. S. Sehar, I. Naz, N. Ali and S. Ahmed, *Environ. Monit. Assess.*, **185**, 1129 (2013); https://doi.org/10.1007/s10661-012-2620-2
65. G.A. Hudson, L. Cheng, J. Yu, Y. Yan, D.J. Dyer, M.E. McCarroll and L. Wang, *J. Phys. Chem. B*, **114**, 870 (2010); https://doi.org/10.1021/jp908368k